

# Structural brain signature of cognitive decline in Parkinson's disease: DTI-based evidence from the LANDSCAPE study

Martin Gorges, Hans-Peter Müller, Inga Liepelt-Scarfone, Alexander Storch, Richard Dodel, LANDSCAPE Consortium, Rüdiger Hilker-Roggendorf, Daniela Berg, Martin S. Kunz, Elke Kalbe, Simon Baudrexel and Jan Kassubek 

## Abstract

**Background:** The nonmotor symptom spectrum of Parkinson's disease (PD) includes progressive cognitive decline mainly in late stages of the disease. The aim of this study was to map the patterns of altered structural connectivity of patients with PD with different cognitive profiles ranging from cognitively unimpaired to PD-associated dementia.

**Methods:** Diffusion tensor imaging and neuropsychological data from the observational multicentre LANDSCAPE study were analyzed. A total of 134 patients with PD with normal cognitive function (56 PD-N), mild cognitive impairment (67 PD-MCI), and dementia (11 PD-D) as well as 72 healthy controls were subjected to whole-brain-based fractional anisotropy mapping and covariance analysis with cognitive performance measures.

**Results:** Structural data indicated subtle changes in the corpus callosum and thalamic radiation in PD-N, whereas severe white matter impairment was observed in both PD-MCI and PD-D patients including anterior and inferior fronto-occipital, uncinate, insular cortices, superior longitudinal fasciculi, corona radiata, and the body of the corpus callosum. These regional alterations were demonstrated for PD-MCI and were more pronounced in PD-D. The pattern of involved regions was significantly correlated with the Consortium to Establish a Registry for Alzheimer's Disease (CERAD) total score.

**Conclusions:** The findings in PD-N suggest impaired cross-hemispherical white matter connectivity that can apparently be compensated for. More pronounced involvement of the corpus callosum as demonstrated for PD-MCI together with affection of fronto-parieto-temporal structural connectivity seems to lead to gradual disruption of cognition-related cortico-cortical networks and to be associated with the onset of overt cognitive deficits. The increase of regional white matter damage appears to be associated with the development of PD-associated dementia.

**Keywords:** dementia, diffusion tensor imaging, magnetic resonance imaging, mild cognitive impairment

Received: 21 October 2018; revised manuscript accepted: 19 March 2019

## Introduction

The recognition that the pathological process underlying sporadic Parkinson's disease (PD) extends far beyond the dopaminergic system<sup>1</sup> has fundamentally changed the understanding of PD pathogenesis and therapeutic options.<sup>2</sup> A broad

spectrum of nonmotor features including cognitive decline accompany the course of PD<sup>3</sup> and impacts health-related quality of life<sup>4</sup> and survival. The Braak hypothesis<sup>1</sup> proposes an ascending pattern of pathology spreading from the lower brain stem (presymptomatic stages 1–2) to

*Ther Adv Neurol Disord*

2019, Vol. 12: 1–15

DOI: 10.1177/  
1756286419843447

© The Author(s), 2019.  
Article reuse guidelines:  
sagepub.com/journals-  
permissions

Correspondence to:

**Jan Kassubek**  
Department of Neurology,  
University of Ulm, RKU,  
Oberer Eselsberg 45, Ulm  
89081, Germany  
[jan.kassubek@uni-ulm.de](mailto:jan.kassubek@uni-ulm.de)

**Martin Gorges**  
**Hans-Peter Müller**  
**Martin S. Kunz**  
Department of Neurology,  
University of Ulm, Ulm,  
Germany

**Inga Liepelt-Scarfone**  
German Center of  
Neurodegenerative  
Diseases and Hertie  
Institute for Clinical Brain  
Research, Tübingen,  
Germany

**Alexander Storch**  
Department of Neurology,  
University of Rostock,  
Rostock, Germany  
Division of  
Neurodegenerative  
Diseases, Department of  
Neurology, Technische  
Universität Dresden,  
Dresden, Germany  
German Centre for  
Neurodegenerative  
Diseases (DZNE) Rostock/  
Greifswald, Rostock,  
Germany

**Richard Dodel**  
Department of Neurology,  
Philipps University  
Marburg, Marburg,  
Germany  
Department of Neuro-  
Geriatrics, University  
Clinic, Essen, Germany

**Rüdiger Hilker-  
Roggendorf**  
Klinik für Neurologie  
und Klinische  
Neurophysiologie,  
Klinikum Vest,  
Knappschafts-Krankenhaus  
Recklinghausen,  
Recklinghausen, Germany

**Daniela Berg**  
German Center of  
Neurodegenerative  
Diseases and Hertie  
Institute for Clinical Brain  
Research, Tübingen,  
Germany

Department of Neurology,  
Christian Albrecht  
University, Kiel, Germany

**Elke Kalbe**  
Medical Psychology |  
Neuropsychology and  
Gender Studies, Center  
for Neuropsychological  
Diagnostics and  
Intervention [CeNDI],  
University Hospital  
Cologne, Cologne,  
Germany

**Simon Baudrexel**  
Department of Neurology,  
J.W. Goethe University,  
Frankfurt/Main, Germany

mesencephalic structures including the substantia nigra (early symptomatic stage 3–4). The development of cognitive deficits<sup>5</sup> is a functional consequence of late symptomatic stages (Braak stages 5–6) when the underlying pathological process finally reaches the neocortex.<sup>6</sup>

The cognitive profile of PD patients spanning from cognitively normal (PD-N) to the transient phase of mild cognitive impairment (PD-MCI) and finally to the full picture of PD-associated dementia (PD-D) has been well defined.<sup>7</sup> Accumulating evidence from neuroimaging studies suggest an abnormal network architecture in PD patients involving frontal and interhemispheric white matter systems which have been shown to be related to cognitive status.<sup>8–11</sup> Diffusion tensor imaging (DTI) is useful for investigating hippocampal connections and frontostriatal circuits that have been discussed to mediate cognitive decline and have been suggested to be a potential candidate as an *in vivo* surrogate marker for cognitive impairment in PD.<sup>12</sup> However, the corresponding patterns of structural abnormalities in neuropsychologically characterized patients with PD and their relations to cognitive performance have not yet been systematically investigated in a homogeneous large cohort including PD-N, PD-MCI, and PD-D subtypes.

The present study aimed to gain mechanistic insights and to put quantitative evidence to the structural imaging correlates of the continuous process of cognitive decline by investigating microstructural changes in a large PD patient sample comprising PD-N, PD-MCI and PD-D. We hypothesized that cognitively unimpaired patients with PD will present with, if at all, mild white matter lesions while patients with cognitive impairment would show a pattern of disrupted connections between mesocortical and neocortical areas (in accordance with the Braak staging model). Next, we hypothesized that correlations with neuropsychological parameters would allow us to identify the signature of microstructural impairment in specific cognitive domains. The hypotheses were tested in a multicentre cohort study of PD patients from the prospective observational LANDSCAPE study, designed to trace the course of PD from cognitively normal to PD-associated dementia.<sup>13</sup> Cross-sectional baseline data sets including DTI data together with a full neuropsychological profile were analyzed.

## Methods

### *The LANDSCAPE baseline cohort*

From the multicentre, prospective, observational LANDSCAPE study,<sup>13</sup> baseline data from 134 PD patients and 72 healthy controls from five national clinical sites (movement disorders centres) were analyzed (Table 1). For inclusion, patients were between 45 and 80 years of age and met the diagnosis of PD according to the UK Parkinson's Disease Society Brain Bank clinical diagnostic criteria.<sup>14</sup> Patients were excluded for the following reasons: (1) diagnosis of or evidence for atypical Parkinson syndromes; (2) other causes of dementia based on clinical grounds; (3) severe cognitive impairment that impedes consent; (4) medical and ethical reasons in relation to the morphological and neurobiological examinations; and (5) pregnancy. Inclusion and exclusion criteria and all assessments including magnetic resonance imaging (MRI) acquisition followed the LANDSCAPE consortium guidelines, for details refer to Balzer-Geldsetzer and colleagues.<sup>13</sup>

All patients included in the LANDSCAPE study provided detailed written and informed consent. The LANDSCAPE study was approved by the Ethics Committee of Philipps University Marburg (approval no. 25/11, 18 October 2011) together with the local ethics committees of all participating centres (Table 1).

### *Clinical and neuropsychological assessment*

Table 2 summarizes demographical, clinical and neuropsychological scales according to the previously published protocol.<sup>13</sup> In brief, demographical features and medication, summarized as levodopa-equivalent daily dose (LEDD), were assessed together with the German versions of the (1) Mini Mental State Examination (MMSE); (2) the Parkinson Neuropsychometric Dementia Assessment (PANDA); and (3) the Consortium to Establish a Registry for Alzheimer's Disease (CERAD) test battery. The CERAD covers the cognitive domains of (1) memory, (2) executive functions, (3) attention, (4) visuospatial functions, and (5) language. The CERAD total score was computed from four cognitive domains including 39% language, 30% learning, 11% construction, and 20% memory as previously described.<sup>15</sup> In particular, the subscores from verbal fluency (domain: language), Boston naming test (language), word list learning (learning), constructional praxis

**Table 1.** Basic demographic features and MR scanning protocols of the multicentre setting. Magnetic resonance data from patients with PD and healthy controls were acquired at five German sites (Dresden, Frankfurt, Marburg, Tübingen, and Ulm). DTI data were transversally recorded in interleaved even order. T<sub>2</sub>-weighted FLAIR were sagittally recorded.

Centre	01	02	03	04	05	p value
PD patients (M/F)	33 (25/8)	27 (18/9)	22 (19/3)	25 (18/7)	27 (18/9)	0.518 <sup>†</sup>
age/y <sup>†</sup>	68 ± 6 (54–78)	67 ± 8 (49–79)	66 ± 9 (48–77)	68 ± 8 (46–79)	68 ± 9 (45–79)	0.048 <sup>†</sup>
Controls (M/F)	14 (7/7)	14 (6/8)	12 (7/5)	13 (6/7)	19 (13/6)	0.593 <sup>†</sup>
age/y <sup>†</sup>	63 ± 8 (49–73)	66 ± 5 (58–78)	62 ± 8 (47–71)	66 ± 6 (58–76)	69 ± 5 (61–79)	0.947 <sup>†</sup>
Vendor	SIEMENS	SIEMENS	SIEMENS	SIEMENS	SIEMENS	
Model	Verio	Trio	TrioTim	TrioTim	Allegra	
Field/T	3.0	3.0	3.0	3.0	3.0	
<b>DTI</b>						
TR/s	12.7	12.7	12.7	12.7	12.7	
TE/ms	81	95	85	86	95	
Flip angle/deg	90	90	90	90	90	
Voxel (x/y/z)/mm <sup>3</sup>	2.0/2.0/2.0	2.0/2.0/2.0	2.0/2.0/2.0	2.0/2.0/2.0	2.0/2.0/2.0	
Gradient directions	62	35	62	62	31	
b/s/mm <sup>2</sup>	1000	1000	1000	1000	1000	
<b>FLAIR</b>						
TR/s	5.0	5.0	5.0	5.0	5.0	
TE/ms	395	335	394	394	355	
Flip angle/deg	120	180	120	120	180	
Voxel (x/y/z)/mm <sup>3</sup>	1.0/1.0/1.0	1.0/1.0/1.0	1.0/1.0/1.0	1.0/1.0/1.0	1.0/1.0/1.0	
<sup>†</sup> Values are given as mean ± standard deviation (min–max). <sup>†</sup> Kruskal–Wallis analysis of variance on ranks. *Chi-square test. DTI, diffusion tensor imaging; F, female; FLAIR, fluid-attenuated inversion recovery; M, male; MR, magnetic resonance; PD, Parkinson's disease; TE, time echo; TR, time repetition.						

(construction), word list recall (memory), and word list recognition discriminability (memory) were summed. Importantly, the resulting interim total score was further corrected for age, sex and education by adding a tabulated correction factor (see online Table E-1 in Chandler and colleagues<sup>15</sup> computed from a regression model). The resulting sociodemographically corrected CERAD total score was subjected to further statistical analyses.

#### Definition of subgroups

The PD cohort of 134 cases comprised 56 PD-N, 67 PD-MCI, and 11 PD-D patients who were classified according to the following criteria: PD-MCI was established according to the MCI criteria<sup>16</sup> and PD-D classification was made according to the Movement Disorder Society Task Force guidelines.<sup>17</sup> A patient was regarded as cognitively impaired when: (1) the patient presented with

**Table 2. Demographic, clinical and neuropsychological characteristics of all patients.** Demographic, clinical, and neuropsychological characteristics of the total PD sample, cognitively normal (PD-N), mildly cognitively impaired (PD-MCI), demented patients (PD-D), and healthy controls. Data are given as mean  $\pm$  standard deviation (min–max) except for sex.

	Healthy controls <i>n</i> = 72	Total PD <i>n</i> = 134 (100%)	<i>p</i> *	PD-N <i>n</i> = 56 (42%)	PD-MCI <i>n</i> = 67 (50%)	PD-D <i>n</i> = 11 (8%)	<i>p</i> value+
Sex M/F	39/33	98/36	0.006	41/15	48/19	9/2	0.046
Age/y	65 $\pm$ 7 (47–79)	67 $\pm$ 8 (45–79)	0.054	66 $\pm$ 8 (45–78)	68 $\pm$ 8 (48–79)	71 $\pm$ 4 (63–76)	0.013
Education/y	16 $\pm$ 4 (10–30)	13 $\pm$ 3 (7–20)	<0.001	13 $\pm$ 3 (8–19)	13 $\pm$ 3 (7–20)	13 $\pm$ 4 (7–11)	<0.001
PD duration / y	NA	9 $\pm$ 4 (0–18)		9 $\pm$ 5 (0–24)	8 $\pm$ 4 (3–16)	12 $\pm$ 4 (5–18)	0.107
LEDD / (mg/d)	NA	663 $\pm$ 426 (0–1686)		624 $\pm$ 420 (0–1686)	640 $\pm$ 410 (0–1541)	1081 $\pm$ 400 (767–1582)	0.007
Hoehn and Yahr stage	NA	2.7 $\pm$ 0.8 (2–4)		2.3 $\pm$ 0.7 (1–4)	2.5 $\pm$ 0.7 (1–5)	3.4 $\pm$ 0.7 (2–4)	<0.001
UPDRS III	NA	22 $\pm$ 11 (5–64)		18 $\pm$ 8 (5–45)	22 $\pm$ 10 (6–55)	40 $\pm$ 13 (19–64)	<0.001
Neuropsychological data							
MMSE	30	28 $\pm$ 2 (21–30)	<0.001	29 $\pm$ 1 (26–30)	28 $\pm$ 2 (22–30)	24 $\pm$ 2 (21–27)	<0.001
PANDA	NA	23 $\pm$ 5 (10–30)		25 $\pm$ 4 (13–30)	22 $\pm$ 5 (10–29)	13 $\pm$ 3 (10–21)	<0.001
CERAD total score†	NA	93 $\pm$ 11 (42–113)		99 $\pm$ 6 (86–113)	91 $\pm$ 8 (70–107)	69 $\pm$ 12 (42–84)	<0.001
-Verbal fluency)‡	NA	-0.2 $\pm$ 1.1 (-3.4–2.5)		0.3 $\pm$ 0.9 (-1.4 to 2.5)	-0.5 $\pm$ 1.1 (-2.5 to 2.3)	-1.7 $\pm$ 0.9 (-3.4 to -0.2)	<0.001
- Boston naming test‡	NA	-0.2 $\pm$ 1.0 (-3.2 to 1.9)		0.5 $\pm$ 0.7 (-0.9 to 1.9)	0.2 $\pm$ 1.0 (-2.5 to 1.5)	-1.4 $\pm$ 0.9 (-3.2 to 0.0)	<0.001
-Word list learning‡	NA	-0.0 $\pm$ 1.2 (-5.0 to 3.1)		0.5 $\pm$ 1.0 (-1.8 to 3.1)	-0.5 $\pm$ 1.4 (-4.6 to 2.8)	-1.9 $\pm$ 1.7 (5.0–2.1)	<0.001
-Word list recall‡	NA	-0.0 $\pm$ 1.2 (-3.9 to 2.8)		0.5 $\pm$ 0.9 (-1.1 to 2.1)	-0.2 $\pm$ 1.1 (2.2–2.8)	-1.6 $\pm$ 1.6 (-3.9 to 1.4)	<0.001
-Word list discrimination‡	NA	-0.1 $\pm$ 1.0 (-2.6 to 1.9)		0.4 $\pm$ 0.8 (-1.8 to 1.9)	-0.0 $\pm$ 1.1 (-2.5 to 1.2)	-1.1 $\pm$ 0.9 (-2.6 to 0.8)	0.005
-Constructional praxis‡	NA	-0.1 $\pm$ 1.3 (-8.3 to 1.5)		0.5 $\pm$ 0.7 (-1.5 to 1.5)	0.1 $\pm$ 1.0 (-2.6 to 1.4)	-2.7 $\pm$ 2.3 (-8.3 to 0.8)	<0.001

†CERAD total score is the sum of six subscores

‡and is sociodemographically corrected for normative data including age, education, and sex.<sup>15</sup>

‡CERAD scores are given as z scores.

\*Unpaired two-sample Student's *t* test for unequal variances for continuous variables and Chi-square test for categorical variables.

+Kruskal–Wallis analysis of variance on ranks for PD-N, PD-MCI, PD-D and healthy controls for continuous variables and Chi-square test for categorical variables.

CERAD, Consortium to Establish a Registry for Alzheimer's Disease; F, female; LEDD, levodopa-equivalent daily dose; M, male; MMSE, mini mental state examination; NA, not available/not applicable; PANDA, Parkinson neuropsychometric dementia assessment;<sup>13</sup> PD, Parkinson's disease; PD-D, patients with PD-associated dementia; PD-MCI, mildly cognitively impaired PD patients; PD-N, patients with PD with normal cognition; UPDRS, unified Parkinson's disease rating scale.

cognitive impairment (either signs or symptoms reported by the patients themselves), and when (2) there was measurable poor cognitive performance (i.e.  $\leq 1.5$  standard deviations below normative mean values in at least one of the diagnostically relevant neuropsychological tests; Table 2). With regard to this cut-off score, exceptions could be made according to the expert's ratings if clinicians found that clear cognitive impairment was evident despite performance above this cut-off score (e.g. in highly educated individuals) or if a performance of a specific patient who scored below this cut-off was still evaluated as 'within normal range' by the person performing the test. The group of PD-MCI patients were categorized depending on their cognitive profile into one of the four MCI subtypes according to the established MCI criteria,<sup>16</sup> [i.e. amnesic MCI-single domain (4.8%), amnesic MCI-multidomain (28.6%), nonamnesic MCI-single domain (54.7%), and nonamnesic MCI-multidomain (11.9%)]. Patients with cognitive impairment who: (1) performed in at least one diagnostically relevant neuropsychological test in at least two cognitive domains below the normative cut-off score, and (2) presented with significant impairment in activities of daily living according to medical history (social, occupational, or personal care) were classified as PD-D.<sup>17</sup>

For group comparisons, age-matched controls were sampled from the overall control cohort ( $n = 72$ ) resulting in three control subgroups including: (1) age-matched controls for PD-N patients ( $n = 56$ ), (2) age-matched controls for PD-MCI patients ( $n = 67$ ), and (3) age- and education-matched controls for PD-D patients ( $n = 22$ ). Demographic and neuropsychological features of the PD subgroups and matched controls are summarized in Supplementary Table 1.

#### *DTI data analysis*

The DTI multicentre data analysis followed a standardized and well-established procedure<sup>18,19</sup> and was performed using the *Tensor imaging and fibre tracking* software package.<sup>20</sup> In brief, DTI processing included: (1) data quality control, (2) normalization to the Montreal Neurological Institute (MNI) stereotaxic standard space (3) fractional anisotropy (FA) map computation, (4) removing of confounding factors, and (5) data pooling in a multicentre framework.<sup>19</sup> Centre-specific details on the DTI protocol and basic demographical features are summarized in Table 1.

#### *Data processing*

In order to minimize partial volume effects,<sup>21</sup> DTI data were upsampled from  $2 \times 2 \times 2 \text{ mm}^3$  into a  $1 \text{ mm}^3$  isogrid (matrix  $256 \times 256 \times 256$ ) using the average voxel intensity of the  $k$ -nearest neighbour voxels weighted by the inverse of their distance. All data were assessed for completeness and subjected to the quality control pipeline.<sup>22</sup> Accordingly, corrupted gradient directions in each individual data sets were discarded<sup>22</sup> and high-order eddy current-induced geometric distortions of the diffusion-weighted echo-planar images were corrected.<sup>23</sup> Our standardized iterative landmark-based deformation approach was used to normalize all volumes into a standard stereotaxic MNI space<sup>24</sup> for all patients; this iterative procedure included the computation of a study-specific template set ( $b_0$  and FA).

#### *DTI metrics map computation*

DTI metrics maps [FA, axial diffusivity (AD), mean diffusivity (MD), and radial diffusivity (RD)] were computed from the MNI normalized data. While FA is sensitive to microstructural changes, it does not indicate a specific type of lesion; on the other hand, among the FA metrics, MD is an inverse measure of the membrane density, AD tends to be strongly affected by axonal injury, while RD increases upon white matter damage due to demyelination and less to changes in the axonal diameters or density.<sup>25-27</sup> Spatial smoothing of DTI metrics maps was performed using a 8 mm, three-dimensional (3D), full-width at half maximum Gaussian blur filter as a common choice according to the matched filter design.

DTI metrics maps were centre-wise corrected for age; scan parameters including voxel size, time echo (TE), number of gradient directions and  $b_0$  were identical between sites (Table 1). Centre-wise pooling of patients' DTI metrics maps was performed by regressing out a 3D centre-specific correction matrix calculated from the centre's controls' data as previously reported.<sup>18,19</sup> Finally, DTI maps of patients and controls were harmonized by application of the respective centre-wise 3D correction matrices (linear first order correction) to the datasets.

#### *Quantification of white matter lesion load*

The white matter lesion load was quantified from T2-weighted fluid-attenuated inversion recovery

(FLAIR) images for all participants (see Table 1 for centre-specific details on the FLAIR sequence). Classification of white matter lesions by grades 0–3 followed the rating scale by Fazekas and colleagues.<sup>28</sup>

#### Statistical data analysis

Sociodemographic, clinical, and neuropsychological data analysis was applied using the MATLAB®-based ‘Statistical Toolbox’ (Mathworks Inc., Natick, MA, USA). Parametric unpaired two-sample Student’s *t* tests for unequal variances were performed to test for differences between two groups, and Kruskal–Wallis analysis of variance (ANOVA) on ranks was performed in the case of three or more groups and were followed in the event of significance by *post hoc* testing using unpaired two-sample Student’s *t* tests for unequal variances. All tests were two-sided, and the *p* value threshold for statistical significance was set to 0.005 for claims of new discoveries.<sup>29</sup>

Voxel-wise statistical comparisons (whole-brain-based spatial statistics; WBSS) of the DTI maps were performed by voxel-wise two-sample Student’s *t* tests for unequal variances, followed by multiple comparisons correction using the false discovery rate (FDR) algorithm at a 5% level using the software package *TIFT*<sup>20</sup>; the DTI metrics maps (i.e. FA, AD, MD, RD) were thresholded for values  $>0.2$ .<sup>30</sup> The cluster size of 256 voxels corresponds to a sphere with a radius of two recording voxels (comparable to the filter size of 8 mm full width at half maximum (FWHM)). To further reduce false-positive findings, a parametric correlation-based clustering procedure that discarded isolated clusters at a threshold cluster size of 256 voxels was applied.<sup>22</sup>

All correlations were analyzed in the group of all PD patients ( $n = 134$ ) using Spearman rank order correlations. Voxel-wise correlations between FA values and cognitive measures (i.e. CERAD total score) resulted in correlations maps (*r* maps) that were subjected to the FDR algorithm at a 5% level, followed by a clustering procedure omitting cluster size below 512 voxels.<sup>22</sup> In addition, significant clusters as revealed from group-wise comparison [i.e. PD patients ( $n = 134$ ) *versus* controls ( $n = 72$ )] were subjected to cluster-wise Spearman rank order correlations to both CERAD total score and to CERAD subscores that included the Boston

naming test, constructional praxis, verbal fluency, word list discrimination, word list learning, and word list recall.

## Results

#### Clinical and cognitive data from the LANDSCAPE cohort

Out of the LANDSCAPE baseline cohort, DTI and sociodemographic, clinical and neuropsychological data of 206 patients from five sites including 134 PD patients and 77 healthy controls (Table 1) were subjected to the whole-brain based analyses of FA maps that were corrected for different centre-dependent protocols and age. The overall cohort of PD patients ( $n = 134$ ) allowed for classification into PD with intact cognition (PD-N,  $n = 56$ , 42%), mild cognitive impairment (PD-MCI,  $n = 67$ , 50%), or dementia (PD-D,  $n = 11$ , 8%); thus ranging from high cognitive performance (e.g. a sociodemographically corrected CERAD total score of 113 and a PANDA score of 29) to the full picture of PD-associated dementia (e.g. CERAD total score 43, PANDA score of 10). All details of subject characterization are summarized in Table 2. Overall cognitive performance as measured by the sociodemographically corrected CERAD total score presented a marked gradient from PD-N patients (score  $99 \pm 6$ ) to PD-MCI (score  $91 \pm 8$ , *versus* PD-N, 8% loss,  $t = 5.84$ ,  $p < 0.0001$ ) and finally to PD-D (score  $69 \pm 12$ , *versus* PD-MCI, 24% loss,  $t = 5.61$ ,  $p < 0.0001$ , *versus* PD-N, 30% loss,  $t = 7.75$ ,  $p < 0.0001$ ). Physical disability was less in PD-N [mean Hoehn and Yahr stage, 2.3; mean unified Parkinson’s disease rating scale (UPDRS) III, 18] than in PD-MCI (Hoehn and Yahr stage, 2.5; mean UPDRS III, 22) and in PD-D (Hoehn and Yahr stage, 3.4; mean UPDRS III, 38). In all PD patients ( $n = 134$ ), the CERAD total scores correlated significantly with motor disability as measured by UPDRS III scores (Spearman rank  $r = -0.31$ ,  $p = 0.0005$ ).

#### Distributed microstructural damage in the overall cohort of PD patients

The WBSS analysis including various DTI metrics (FA, AD, MD, RD) in all patients with PD (PD-N, PD-MCI, and PD-D patients) compared with controls revealed a widespread pattern of significant white matter lesions involving mainly the mesocortical connections and mesencephalic structures, while the neocortical

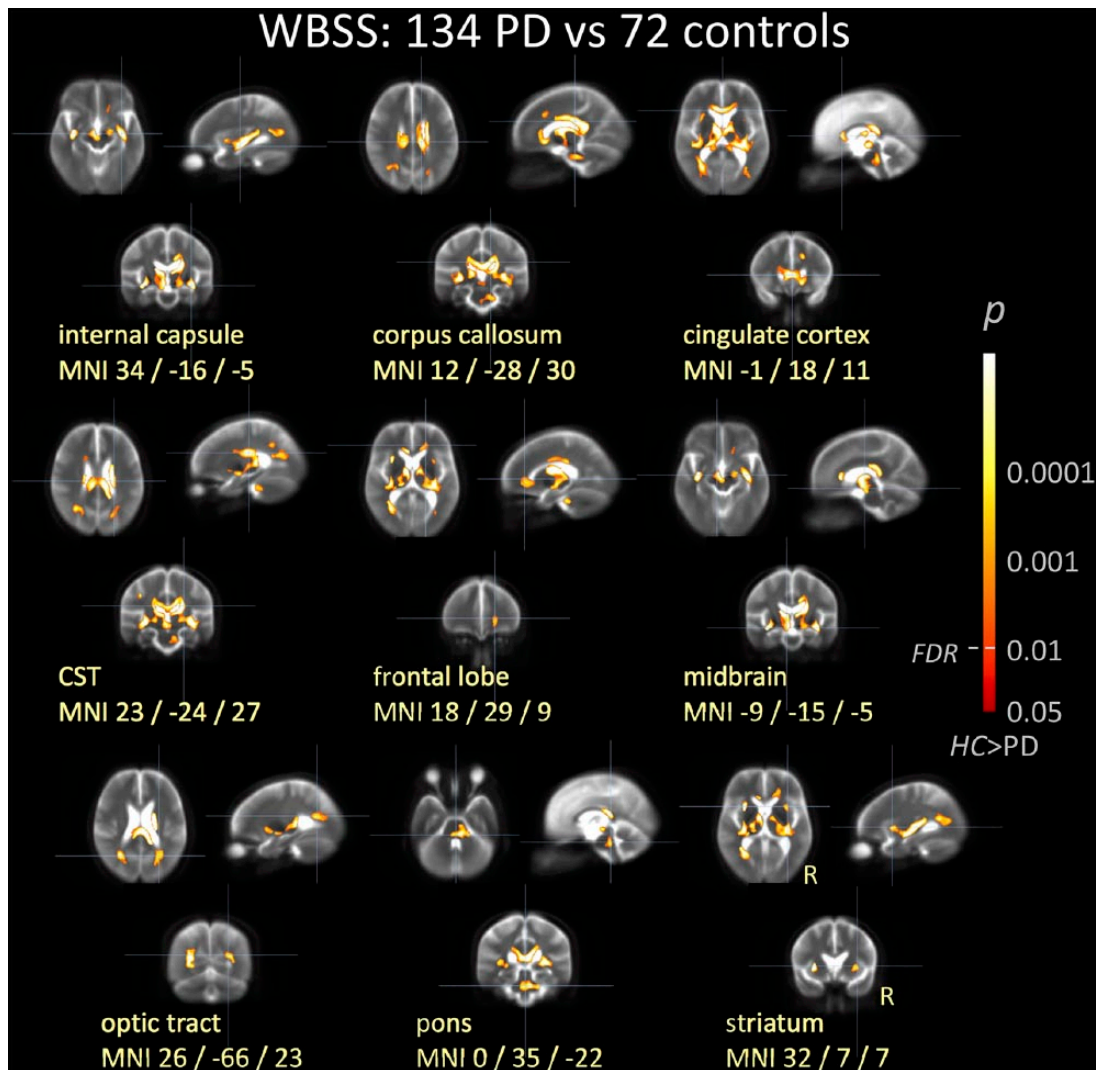


**Figure 1.** WBSS of the FA maps showing results of group comparison for PD patients compared with healthy controls.

Hot colours indicate cluster of significant reduction of FA in PD patients after correction for confounding multicentric factors ( $p < 0.01$ , FDR corrected with further cluster-wise correction to reduce false-positive errors). Shown are triplets of most representative orthogonal slices displayed on a multicentre study-specific averaged  $b_0$ -template as background.

FA, fractional anisotropy; FDR, false discovery rate; MNI, Montreal Neurological Institute; PD, Parkinson's disease; WBSS, whole-brain-based spatial statistics.

connections presented only mild affection (Figure 1 and Supplementary Figure 1). In particular, FA was significantly decreased in the corona radiata, body of the corpus callosum, anterior, inferior and superior fasciculus, cingulum, corticospinal tract, insular cortex, and thalamic radiation ( $p < 0.01$ , FDR corrected, cluster-wise corrected). AD was increased in the internal capsule, the body of the corpus callosum, and in the corticospinal tract, MD was increased in the internal capsule, the body of the corpus callosum, in the corticospinal tract, the

cingulate cortex, the frontal lobe, the optic tract, and in the striatum (all of these structures showed a decrease in FA), and RD was increased in the internal capsule, and in the corticospinal tract. No RD increase was observed in the corpus callosum. In Figure 2, the PD subgroups (11 PD-N, 67 PD-MCI, and 56 PD-D) were compared with the complete controls group ( $n = 72$ ). In order to demonstrate consistency for matched groups, Supplementary Figure 2 demonstrates similar results also for matched controls groups.

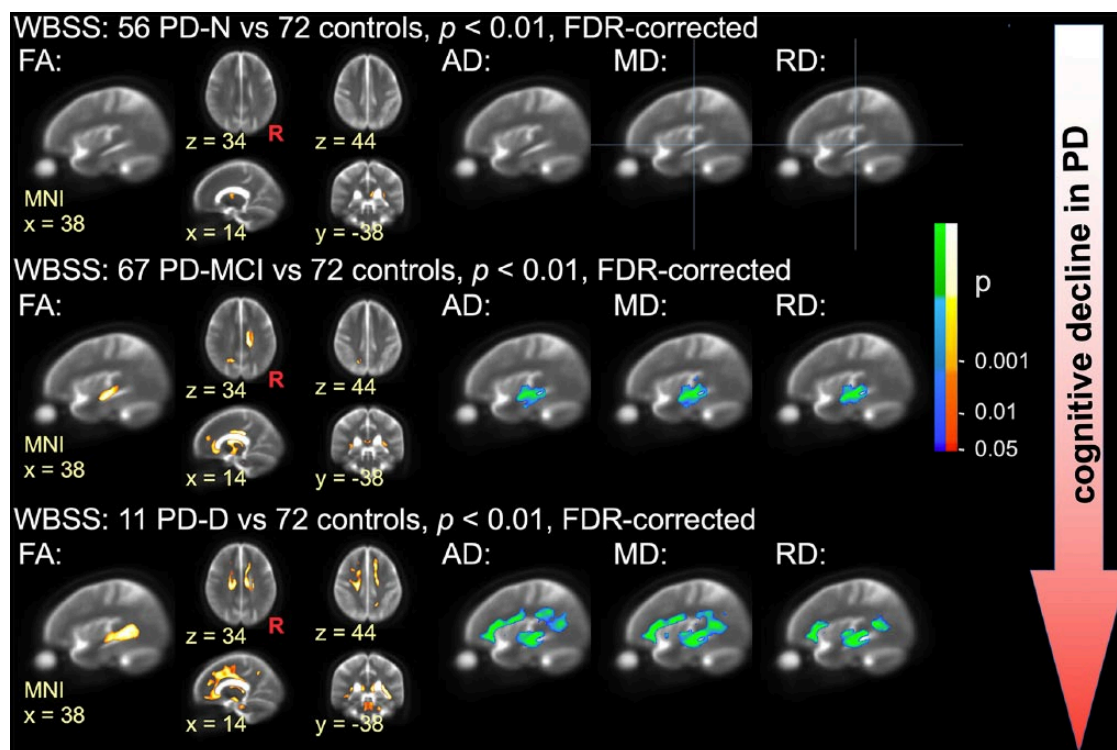


**Figure 2.** WBSS of DTI metrics in different cognitive PD subtypes compared with healthy controls. Hot colours indicate clusters of significant decrease of FA (left columns) in patients with PD with normal cognition (PD-N; upper row), mildly cognitively impaired PD patients (PD-MCI, centre row), and patients with PD-associated dementia (PD-D; lower row). Cool colours indicate clusters of significant increase of AD, MD, and RD in PD-N patients, PD-MCI patients, and PD-D patients (right columns, MNI  $x = 38$ ). All results are shown for  $p < 0.01$  with FDR correction and with further cluster-wise correction. Images are representative orthogonal slices displayed on a study-specific averaged  $b_0$ -template as the background.

AD, axial diffusivity; DTI, diffusion tensor imaging; FA, fractional anisotropy; FDR, false discovery rate; MD, mean diffusivity; MNI, Montreal Neurological Institute, PD, Parkinson's disease; PD-D, patients with PD-associated dementia; PD-MCI, mildly cognitively impaired PD patients; PD-N, patients with PD with normal cognition; R, right hemisphere; RD, radial diffusivity; WBSS, whole-brain-based spatial statistics.

#### *Involvement of the limbic lobe and striatal circuit in cognitively normal PD*

Compared with controls, PD patients with neuropsychologically confirmed 'normal' cognition, (i.e. PD-N patients) showed significantly altered DTI metrics including FA, AD, MD, and RD values in the body of the corpus callosum and the thalamocortical radiations bilaterally ( $p < 0.01$ , FDR corrected, cluster-wise corrected), indicating an early involvement of the striatal circuit and specifically of the pathways projecting back to the motor cortex (upper panels in Figure 2 and Supplementary Figure 1). No significant changes in DTI metrics were found in the entire neocortical connections, and FA decreases and AD, MD, and RD changes were limited to subcortical structures.

#### *Involvement of mesocortical and cortical projection fibres in PD-MCI*

Compared with controls, PD-MCI was accompanied with significantly altered DTI metrics including FA, AD, MD, and RD values in the thalamus and the corpus callosum (centre panels in Figure 2 and Supplementary Figure 1). In addition, the pattern of significant FA decreases also involved the striatum, the cingulum, anterior and superior corona radiata, anterior, inferior and superior fasciculi, corticospinal tract, and insular connections. The direct comparison within patient subgroups, (i.e. PD-MCI *versus* PD-N patients), confirmed the marked white matter involvement in PD-MCI with decreased FA mainly in the inferior longitudinal fasciculus at FDR corrected, cluster-wise corrected  $p < 0.01$  [see also Figure 3(a), upper panel].



## WBSS in 134 PD patients and correlations with cognitive performance

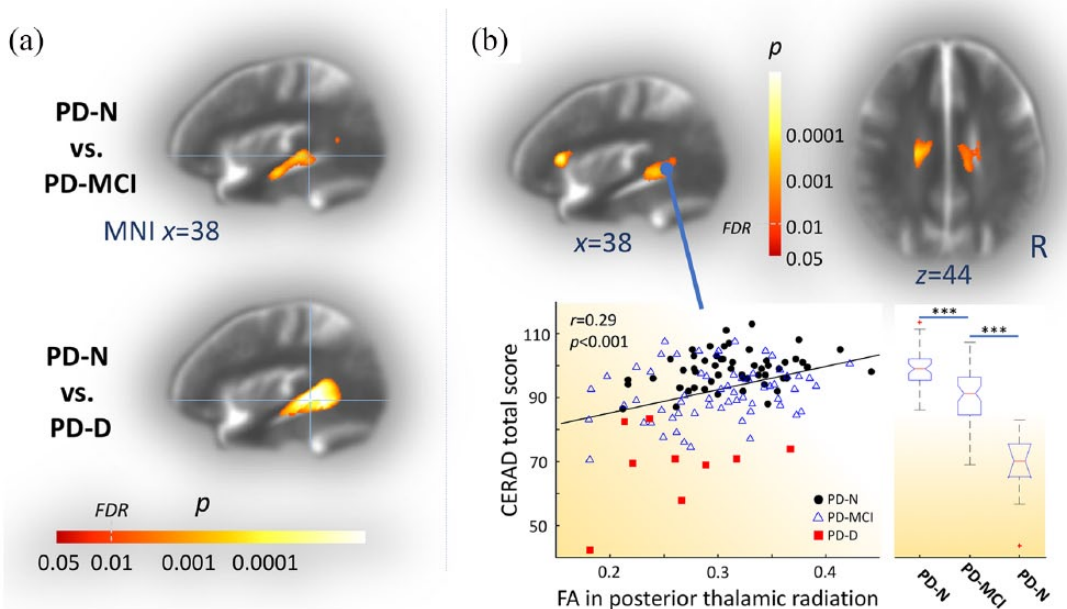


**Figure 3.** WBSS of the FA map and correlations with cognitive scores.

(a) WBSS of the FA maps showing results of cognitively impaired PD subtypes compared with cognitively normal cases (PD-N). Hot colours indicate a cluster of significant decrease of FA in mildly cognitively impaired patients with PD (PD-MCI, upper panel) and patients with PD-associated dementia (PD-D, lower panel). (b) Voxel-wise correlation maps showing hot colours coding significant Spearman rank order correlation coefficients ( $p < 0.01$ , FDR corrected, cluster-wise corrected for further reduction of the alpha error) between FA values of all patients with PD and the sociodemographically corrected CERAD total scores (upper row). Scatter plot in lower right panel exemplifies significant correlation ( $r = 0.29$ ,  $p < 0.001$ ) for a representative spherical ROI ( $r = 5$  mm) with the centre at [MNI  $x/y/z = 38/-90/2$ ] illustrating FA/CERAD total score pairs for PD-N (black dots), PD-MCI (blue triangles), and PD-D patients (red squares). Box plots (lower left panel) indicated a marked gradient of overall cognitive performance decline from PD-N, along PD-MCI towards PD-D as measured by the sociodemographically corrected CERAD total score [pairwise Student's  $t$  test,  $***p < 0.001$ ]. (a, b) Group comparisons and correlation patterns were computed for FA values after correction for confounding multicentric factors at  $p < 0.01$ , FDR corrected followed by cluster-wise correction to reduce false-positive errors by discarding small cluster. Shown are most representative orthogonal slices displayed on a multicentre study-specific averaged  $b_0$ -template as background. CERAD, Consortium to Establish a Registry for Alzheimer's Disease; DTI, diffusion tensor imaging; FA, fractional anisotropy; FDR, false discovery rate; MNI, Montreal Neurological Institute, PD, Parkinson's disease; PD-D, patients with PD-associated dementia; PD-MCI, mildly cognitively impaired PD patients; PD-N, patients with PD with normal cognition; ROI, region-of-interest; WBSS, whole-brain-based spatial statistics.

### Pronounced cortical white matter involvement in PD-associated dementia

More widespread white matter alterations including FA, AD, MD, and RD values were observed in the PD-D patients. Here, in addition to the significantly altered DTI metrics compared with controls in all tracts that were found in the PD-MCI cohort (*versus* controls), the pattern of white matter involvement involved the cortical projection fibres mainly in the superior corona radiata (lower panels in Figure 2 and Supplementary Figure 1). From a methodological perspective, it is of note that the PD-D group was of limited size (11 cases) compared with the much larger samples of PD-N ( $n = 56$ ) and PD-MCI ( $n = 67$ ). In order to validate

these findings, group contrasts in all DTI metrics were computed for PD-D patients ( $n = 11$ ) against an age- and education-matched control group ( $n = 22$ ) out of the  $n = 72$  control sample (Supplementary Table 1 for details of this matched control cohort). The results demonstrated that the effect of higher age and less education years in PD-D patients compared with the overall control cohort are negligibly small (Supplementary Figure 1 and Supplementary Figure 1). Very pronounced white matter involvement as demonstrated for PD-D patients *versus* controls (Figure 2, lower row) could be shown in the group comparison within the patient cohort, (i.e. comparing PD-N and PD-D patients), which mainly indicated

significant FA decrease in the superior longitudinal fasciculus [see also Figure 3(a), lower panel]. In summary, the pronounced white matter involvement in PD-D patients mainly affects cortico-cortical connections together with cross-hemispherical structural pathways as well as afferent and efferent projection fibres to the cortex.

#### *No difference in white matter lesion load across groups*

The quantified white matter lesion load following the procedure as suggested by Fazekas and colleagues<sup>28</sup> revealed an average grade of  $1.4 \pm 0.6$  for PD-N patients ( $n = 56$ ),  $1.6 \pm 0.7$  for PD-MCI patients ( $n = 67$ ),  $1.8 \pm 0.8$  for PD-D patients ( $n = 11$ ), and  $1.4 \pm 0.5$  for controls ( $n = 72$ ). White matter lesion load shows a trend to increase with cognitive decline, a tendency that is not significant across groups (Kruskal–Wallis ANOVA on ranks  $df = 3$ ,  $\chi^2 = 6.77$ ,  $p = 0.08$ ) but more likely to be explained by age-related effects (significant correlation in controls  $r = 0.36$ ,  $p = 0.002$ ) in the older PD-MCI group (mean age 68 years) and PD-D group (71 years) as compared with controls (67 years).

#### *White matter pathology correlates with cognitive decline*

The WBSS analyses in PD-MCI and PD-D compared with controls indicated significantly decreased FA values in cognition-related neocortical fibre tracts including afferent and efferent projection fibres (Figure 2). Spearman rank order correlation analyses across all PD patients ( $n = 134$ ) revealed significant correlations between cognitive state-dependent regional FA changes and the sociodemographically corrected CERAD total score in the insular cortex, superior longitudinal fasciculus, posterior and superior corona radiata, body of the corpus callosum, and cingulum [Spearman rank order  $r > 0.25$ ,  $p < 0.01$ , FDR corrected, cluster-wise corrected; Figure 3(b)]. However, voxel-wise correlation analysis between FA values and CERAD subscores including the Boston naming test, constructional praxis, verbal fluency, word list discrimination, word list learning, and word list recall, respectively, revealed no significant findings. Finally, we studied cluster-wise correlations for all clusters indicating significant microstructural changes that resulted from group comparisons of DTI metrics including FA, AD, MD, RD between all

PD patients ( $n = 134$ ) and controls ( $n = 72$ ). Consistently, cluster-wise correlations of DTI metrics including AD, MD, and RD confirmed the association between CERAD performance and impairment in the internal capsule, cingulate cortex, CST, and CC (Supplementary Table 2), similar to FA voxel-wise correlations. Cluster-wise correlations of AD, MD, and RD revealed significant correlations between CERAD subscores including the Boston naming test, constructional praxis, and verbal fluency and mainly with microstructural impairment of the internal capsule (Supplementary Table 2).

#### **Discussion**

Using DTI data from a large cohort of patients with PD with cognitive profiles ranging from cognitively normal to PD-associated dementia, we demonstrated mild subcortical microstructural impairment in cognitively normal cases (mainly affecting the striatal loop in the bilateral thalamo-cortical radiations) and widespread white matter impairment involving the frontal neocortical connections and large parts of the mesocortical fibres in cognitively impaired patients. The pattern of microstructural involvement in cognition-related fibre bundles forming cortico-cortical, cortico-striatal and cortico-thalamic connections was associated with worse cognitive performance. Those *in vivo* are in full agreement with the postmortem Braak staging hypothesis<sup>1</sup> that demonstrates a nonrandom propagation of PD-pathology<sup>1,31</sup> and neocortical involvement in the final symptomatic stages of PD in association with cognitive decline.<sup>32</sup>

#### *Microstructural changes and cognitive decline*

Microstructural impairment in cognitively normal PD patients has not been reported by other DTI studies<sup>9,11</sup> who used a tract-based spatial statistics approach. However, their findings are consistent with our data for cortical areas, whereas our WBSS approach revealed focal microstructural damage mainly in the thalamic radiation and corpus callosum. Involvement of the thalamic radiation indicates an impaired striatal loop at the functional level, consistent with motor symptoms defining the symptomatic stage of the disease.<sup>33</sup> The impairment of the corpus callosum points towards affected interhemispheric connectivity that possibly shapes the onset of cognitive deficits, as indicated by the correlations with cognitive performance loss. A straightforward conclusion from these results might

be the assumption of adaptive mechanisms that fully compensate mild damage in the corpus callosum. Moreover, one may hypothesize that beginning structural impairment is not yet severe enough to cause cognitive decline evident by performance below the detectable threshold of impairment in PD-N. This statement receives support from ‘resting-state’ functional connectivity data from the LANDSCAPE study in a monocentric cohort of 31 PD patients.<sup>34</sup> First, functional connectivity in cognitively normal PD patients within cognition-related functional networks (e.g. default-mode network) was increased which is most likely an adaptive functional re-organizing mechanism that aims at compensation for ongoing cell loss.<sup>35</sup> Second, functional connectivity in disease-related networks was decreased in cognitively impaired PD patients mainly along the fronto-cingulo-midline cores. In a second study on this subcohort, it could be demonstrated that this pattern of reduced functional connectivity was positively correlated with cognitive performance.<sup>36</sup> The present data provide a possible structural correlate to these findings from ‘resting-state’ functional magnetic resonance imaging (fMRI) data.

Involvement of the corpus callosum was observed to be more pronounced in PD-MCI. Interestingly, according to our data, white matter damage in the superior corona radiata and the cingulum seems to correspond to the observed functional connectivity loss between frontal and posterior brain regions. White matter lesions in fronto-temporo-parietal fibre bundles have been consistently reported in PD-MCI<sup>9</sup> which is linked to a disrupted structural network as demonstrated by a connectome-based study<sup>11</sup> PD-D patients revealed a more pronounced pattern of white matter involvement especially in fronto-temporo-parietal fibre bundles as compared with the white matter involvement in PD-MCI patients, a finding which is in line with a recently published DTI study in PD-D patients.<sup>37</sup>

As indicated by the correlation analysis and the WBSS analysis in different PD cognitive performers, fronto-temporo-parietal structural connections together with the fronto-insular regions appear to critically contribute to the development of cognitive decline. These findings received support from previous findings in PD-MCI patients with reduced functional connectivity between the cores of the dorsal attention network and right fronto-insular regions in MCI patients that were

associated with worse performance in attention/executive functions.<sup>38</sup>

What ultimately pushes the patients across a barrier of detectable cognitive decline? The risk of developing cognitive deficits increases with disease progression<sup>32</sup> and, according to our data, cognitive impairment, apparently becomes evident when critical white matter damage has been reached and compensation is no longer possible. Cerebrovascular white matter lesions negatively impact cognitive performance.<sup>39</sup> Hence, we quantified the cerebrovascular lesion load in this study and demonstrated no differences in PD-N, PD-MCI, and PD-D groups as compared with controls. This result suggests that the vascular lesion load can be assumed not to confound the analyses and that PD-associated pathology is most likely the main driving factor of the observed cognitive deficits.

The present data support that the affection of fronto-parietal pathways mainly including the superior corona radiata and cingulum is associated with a decline in cognitive performance that becomes worse with a more pronounced involvement of fronto-parieto-temporal pathways as demonstrated for the superior fasciculus in cognitively impaired PD. With respect to the Braak staging hypothesis,<sup>1</sup> cognitive impairment in PD is a clinical consequence in stage 5 and 6 when pathology reaches the mesocortex and association neocortex including high-order sensory association areas and prefrontal fields. Therefore, PD-associated dementia is attributable to stage 5 with involvement of the neocortex affecting additionally primary and secondary motor areas.<sup>31</sup>

Studies suggest the impairment of the ‘cognitive’ striatal loop projecting from the dorsolateral prefrontal cortex to the striatum to be associated with early dysexecutive functions in PD.<sup>40,41</sup> The selective neuronal vulnerability in PD targets only a few susceptible neurons<sup>6</sup> which gradually disrupts structural network connectivity most likely affecting the ‘connections’ rather than the hubs themselves. The decline of structural connections caused by microstructural alterations are too narrow to explain the picture of severe cognitive difficulties.<sup>42</sup> However, the disruption of cortico-cortical networks is associated with cognitive deficits and has been evidenced by graph-based measures in cognitively normal and PD-MCI patients.<sup>11</sup> Despite mild white matter

changes in the absence of cognitive deficits as seen for PD-N patients, it has been recently demonstrated that the overall structural organization remains intact in an early phase of PD, but functional modular organization dramatically changes later in the disease.<sup>43,44</sup>

#### *Limitations and caveats*

A limitation of this study is that the assignment of patients with PD to either the PD-N or PD-MCI group was not based on the recently proposed The International Parkinson and Movement Disorder Society (MDS) criteria<sup>45</sup> as these diagnostic criteria for PD-MCI were not available at study set-up.<sup>13</sup> Thus, the proportion of PD-N and PD-MCI might be slightly different when applying the MDS criteria with which fewer patients would have been assigned to the PD-MCI category,<sup>7</sup> due to the fact that abnormal performance in two tests within each of the five cognitive domains are required to fulfil the level II diagnostic MDS criteria<sup>45</sup> in comparison with the criteria used in this study, (i.e. scores  $\leq 1.5$  SD below normative mean values in at least one of the cognitive tests are required to fulfil the MCI diagnosis).<sup>16</sup> Since the MDS criteria are also dependent on either the patient or informant or a clinician (according to the ‘inclusion criteria’), a retrospective re-evaluation of the PD-MCI would have been confounded by the nonstandardized (subjective) clinician's rating at each site. Nevertheless, as the impact of different criteria is important and will influence the interpretation of the results of our and also other studies, the DEMPARK/LANDSCAPE consortium will present a separate analysis on this aspect (then using the language items of the MMSE as the second ‘language assessment’). Finally, we would like to emphasize that, despite the shortcoming of not using the PD-MCI criteria, we are convinced that our study is able to provide valuable data to the field, because data can be compared with other important large studies on PD-MCI which, for example, used mean  $z$  scores for each cognitive domain which partly relied on only one test.<sup>46,47</sup> Although the number of included cases is large, the study included a limited number of fully demented cases (PD-D,  $n = 11$ ) which does not allow a sufficient characterization of white matter impairment as compared with the sufficiently powered cohorts of PD-MCI and PD-N patients. However, due to a high physical burden that accompanies cognitive decline, the imaging data

from further PD-D cases were in particular confounded by motion artefacts or it was simply impossible to perform the MRI scan for ethical reasons. The various centre-specific confounding MRI acquisition factors were controlled for; however, the possibly negative impact of different MR scanner vendors may still remain a concern.

Another limitation of the DEMPARK/LANDSCAPE study design is that the healthy controls received a limited neuropsychological assessment. However, although the MMSE has limited sensitivity to detect MCI, it seems safe to consider that all controls performing better than 27 points in the MMSE are unlikely to have cognitive deficits. Moreover, the available healthy controls from the LANDSCAPE database differ from PD patients in age and years of education. The higher controls’ education level compared with the PD patients is a potential confounding factor since it is possibly associated with a higher patient-dependent cognitive reserve and with a higher ability to compensate for brain alterations.<sup>48</sup> The possible impact of age on the DTI data was minimized by first, matching a subsample of the healthy controls to each of the patient groups, and second, performing a centre-wise age correction. Importantly, the level of education was similar between the PD subgroups.

#### *Perspective*

Future connectivity analyses in PD may progress towards the emerging *in vivo* concept of jointly studying the underlying neuropathology by the continuous formation of  $\alpha$ -synuclein immunoreactive inclusion bodies<sup>49</sup> and brain connectomics.<sup>50</sup> This concept paves an important future avenue of understanding models of  $\alpha$ -synuclein ‘trafficking’ and the substrate of (mal)functioning of interconnected networks. Unlike Tau-pathology which can be imaged using Tau-positron emission tomography (PET), the development of a corresponding  $\alpha$ -synuclein PET tracer remains to be established. Still, regional FA changes as detectable by DTI can give clues for hot spots of focal white matter damage due to PD-associated pathology.<sup>51,52</sup> Utilized graph-based connectivity analyses of structural connectivity data in association with WBSS may allow to investigate whether a strong region-specific relation of regional white matter damage directly impacts decreased coupling of a coinciding network hub, as recently demonstrated for Alzheimer’s disease.<sup>53</sup> Following this

hypothesis, it remains to be investigated whether the opposite reorganization of the connectivity graph can be demonstrated in PD where higher levels of microstructural focal damage strengthen network connections.

### Conclusions

The results of this study suggest that mildly affected cross-hemispherical connectivity can be compensated up to a point where involvement of the corpus callosum becomes more pronounced together with affection of long-range fronto-parieto-temporal structural connectivity such that cognitive impairment gets clinically recognisable. This leads to gradual disruption of cognition-related cortico-cortical networks which may be associated with cognitive decline and the onset of the transient phase of MCI. When the pathological process finally affects more dorsal regions with more pronounced involvement of fronto-parieto-temporal fibre bundles, the full picture of PD-associated dementia becomes overt. *In vivo* tracing the neuropathological progression together with cognitive performance may provide further achievements on a more detailed understanding of PD-associated pathophysiology. The definition of parameters that may eventually allow for tracing and even predicting the course of PD will particularly impact the landscape of urgently required biomarkers for clinical trials. Moving forward in the field on how structural impairment shapes cognitive performance may eventually guide in the development of the yet limited therapeutic options.

### Acknowledgements

Data were generated within the LANDSCAPE study (representatives: Dr S. Baudrexel, Prof. Dr R. Dodel, Prof. Dr D. Berg, Prof. Dr R. Hilker-Rogendorf, Prof. Dr E. Kalbe, Prof. Dr J. Kassubek, Prof. Dr Klockgether, Dr Liepelt-Scarfone, Prof. Dr B. Mollenhauer, Prof. Dr J. Schulz, Dr A. Spottke, Prof. Dr A. Storch, and Prof. Dr H.-U. Wittchen).

### Funding

The LANDSCAPE study is part of the Competence Network Degenerative Dementias (KNDD) which was funded by the German Federal Ministry of Education and Research (project number 01GI1008C). We are indebted to all staff members in the recruiting centres who contributed to the study.

### Conflict of interest statement

The authors declare that there is no conflict of interest.

### Supplemental material

Supplemental material for this article is available online.

### ORCID iD

Jan Kassubek  <https://orcid.org/0000-0002-7106-9270>

### References

1. Braak H and Del Tredici K. Neuroanatomy and pathology of sporadic Parkinson's disease. *Adv Anat Embryol Cell Biol* 2009; 201: 1–119.
2. Schapira AHV, Olanow CW, Greenamyre JT, *et al.* Slowing of neurodegeneration in Parkinson's disease and Huntington's disease: future therapeutic perspectives. *Lancet* 2014; 384: 545–555.
3. Kalia LV and Lang AE. Parkinson's disease. *Lancet* 2015; 386: 896–912.
4. Duncan GW, Khoo TK, Yarnall AJ, *et al.* Health-related quality of life in early Parkinson's disease: the impact of nonmotor symptoms. *Mov Disord* 2014; 29: 195–202.
5. Litvan I, Aarsland D, Adler CH, *et al.* MDS task force on mild cognitive impairment in Parkinson's disease: critical review of PD-MCI. *Mov Disord* 2011; 26: 1814–1824.
6. Surmeier DJ, Obeso JA and Halliday GM. Selective neuronal vulnerability in Parkinson disease. *Nat Rev Neurosci* 2017; 18: 101–113.
7. Kalbe E, Rehberg SP, Heber I, *et al.* Subtypes of mild cognitive impairment in patients with Parkinson's disease: evidence from the LANDSCAPE study. *J Neurol Neurosurg Psychiatry* 2016; 87: 1099–1105.
8. Cochrane CJ and Ebmeier KP. Diffusion tensor imaging in parkinsonian syndromes: a systematic review and meta-analysis. *Neurology* 2013; 80: 857–864.
9. Agosta F, Canu E, Stefanova E, *et al.* Mild cognitive impairment in Parkinson's disease is associated with a distributed pattern of brain white matter damage. *Hum Brain Mapp* 2014; 35: 1921–1929.
10. Atkinson-Clement C, Pinto S, Eusebio A, *et al.* Diffusion tensor imaging in Parkinson's disease:

- review and meta-analysis. *Neuroimage Clin* 2017; 16: 98–110.
11. Galantucci S, Agosta F, Stefanova E, *et al.* Structural brain connectome and cognitive impairment in Parkinson disease. *Radiology* 2017; 283: 515–525.
  12. Duncan GW, Firbank MJ, O'Brien JT, *et al.* Magnetic resonance imaging: a biomarker for cognitive impairment in Parkinson's disease? *Mov Disord* 2013; 28: 425–438.
  13. Balzer-Geldsetzer M, da Costa ASFB, Kronenbürger M, *et al.* Parkinson's disease and dementia: a longitudinal study (DEMPARK). *Neuroepidemiology* 2011; 37: 168–176.
  14. Hughes AJ, Daniel SE, Kilford L, *et al.* Accuracy of clinical diagnosis of idiopathic Parkinson's disease: a clinico-pathological study of 100 cases. *J Neurol Neurosurg Psychiatry* 1992; 55: 181–184.
  15. Chandler MJ, Lacritz LH, Hynan LS, *et al.* A total score for the CERAD neuropsychological battery. *Neurology* 2005; 65: 102–106.
  16. Petersen RC. Mild cognitive impairment as a diagnostic entity. *J Intern Med* 2004; 256: 183–194.
  17. Emre M, Aarsland D, Brown R, *et al.* Clinical diagnostic criteria for dementia associated with Parkinson's disease. *Mov Disord* 2007; 22: 1689–1707.
  18. Roskopf J, Müller H-P, Dreyhaupt J, *et al.* Ex post facto assessment of diffusion tensor imaging metrics from different MRI protocols: preparing for multicentre studies in ALS. *Amyotroph Lateral Scler Frontotemporal Degener* 2015; 16: 92–101.
  19. Müller H-P, Turner MR, Grosskreutz J, *et al.* A large-scale multicentre cerebral diffusion tensor imaging study in amyotrophic lateral sclerosis. *J Neurol Neurosurg Psychiatry* 2016; 87: 570–579.
  20. Müller H-P, Unrath A, Ludolph AC, *et al.* Preservation of diffusion tensor properties during spatial normalization by use of tensor imaging and fibre tracking on a normal brain database. *Phys Med Biol* 2007; 52: N99–N109.
  21. Müller H-P, Kassubek J, Vernikouskaya I, *et al.* Diffusion tensor magnetic resonance imaging of the brain in APP transgenic mice: a cohort study. *PLoS One* 2013; 8: e67630.
  22. Müller H-P, Kassubek J, Grön G, *et al.* Impact of the control for corrupted diffusion tensor imaging data in comparisons at the group level: an application in Huntington disease. *Biomed Eng Online* 2014; 13: 128.
  23. Shen Y, Larkman DJ, Counsell S, *et al.* Correction of high-order eddy current induced geometric distortion in diffusion-weighted echo-planar images. *Magn Reson Med* 2004; 52: 1184–1189.
  24. Brett M, Johnsrude IS and Owen AM. The problem of functional localization in the human brain. *Nat Rev Neurosci* 2002; 3: 243–249.
  25. Winklewski PJ, Sabisz A, Naumczyk P, *et al.* Understanding the physiopathology behind axial and radial diffusivity changes-what do we know? *Front Neurol* 2018; 9: 92.
  26. Song S-K, Sun S-W, Ramsbottom MJ, *et al.* Demyelination revealed through MRI as increased radial (but unchanged axial) diffusion of water. *Neuroimage* 2002; 17: 1429–1436.
  27. Wang Y, Sun P, Wang Q, *et al.* Differentiation and quantification of inflammation, demyelination and axon injury or loss in multiple sclerosis. *Brain* 2015; 138: 1223–1238.
  28. Fazekas F, Chawluk JB, Alavi A, *et al.* MR signal abnormalities at 1.5 T in Alzheimer's dementia and normal aging. *AJR Am J Roentgenol* 1987; 149: 351–356.
  29. Benjamin DJ, Berger JO, Johannesson M, *et al.* Redefine statistical significance. *Nat Hum Behav* 2018; 2: 6–10.
  30. Kunitatsu A, Aoki S, Masutani Y, *et al.* The optimal trackability threshold of fractional anisotropy for diffusion tensor tractography of the corticospinal tract. *Magn Reson Med Sci* 2004; 3: 11–17.
  31. Del Tredici K and Braak H. Review: Sporadic Parkinson's disease: development and distribution of  $\alpha$ -synuclein pathology. *Neuropathol Appl Neurobiol* 2016; 42: 33–50.
  32. Braak H, Rüb U and Del Tredici K. Cognitive decline correlates with neuropathological stage in Parkinson's disease. *J Neurol Sci* 2006; 248: 255–258.
  33. Silkis I. The cortico-basal ganglia-thalamocortical circuit with synaptic plasticity. II. Mechanism of synergistic modulation of thalamic activity via the direct and indirect pathways through the basal ganglia. *Biosystems* 2001; 59: 7–14.
  34. Gorges M, Müller H-P, Lulé D, *et al.* To rise and to fall: functional connectivity in cognitively normal and cognitively impaired patients with Parkinson's disease. *Neurobiol Aging* 2015; 36: 1727–1735.
  35. Hillary FG and Grafman JH. Injured brains and adaptive networks: the benefits and costs of

- hyperconnectivity. *Trends Cogn Sci (Regul Ed)* 2017; 21: 385–401.
36. Gorges M, Müller H-P, Lulé D, *et al.* The association between alterations of eye movement control and cerebral intrinsic functional connectivity in Parkinson's disease. *Brain Imaging Behav* 2016; 10: 79–91.
  37. Chondrogiorgi M, Astrakas LG, Zikou AK, *et al.* Multifocal alterations of white matter accompany the transition from normal cognition to dementia in Parkinson's disease patients. *Brain Imaging Behav*. In press. DOI: 10.1007/s11682-018-9863-7.
  38. Baggio H-C, Segura B, Sala-Llonch R, *et al.* Cognitive impairment and resting-state network connectivity in Parkinson's disease. *Hum Brain Mapp* 2015; 36: 199–212.
  39. Pinkhardt EH, Issa H, Gorges M, *et al.* Do eye movement impairments in patients with small vessel cerebrovascular disease depend on lesion load or on cognitive deficits? A video-oculographic and MRI study. *J Neurol* 2014; 261: 791–803.
  40. Alexander GE and Crutcher MD. Functional architecture of basal ganglia circuits: neural substrates of parallel processing. *Trends Neurosci* 1990; 13: 266–271.
  41. Kehagia AA, Barker RA and Robbins TW. Cognitive impairment in Parkinson's disease: the dual syndrome hypothesis. *Neurodegener Dis* 2013; 11: 79–92.
  42. Gallagher C, Bell B, Bendlin B, *et al.* White matter microstructural integrity and executive function in Parkinson's disease. *J Int Neuropsychol Soc* 2013; 19: 349–354.
  43. Shah A, Lenka A, Saini J, *et al.* Altered brain wiring in Parkinson's disease: a structural connectome-based analysis. *Brain Connect* 2017; 7: 347–356.
  44. Tinaz S, Lauro PM, Ghosh P, *et al.* Changes in functional organization and white matter integrity in the connectome in Parkinson's disease. *Neuroimage Clin* 2017; 13: 395–404.
  45. Litvan I, Goldman JG, Tröster AI, *et al.* Diagnostic criteria for mild cognitive impairment in Parkinson's disease: Movement Disorder Society Task Force guidelines. *Mov Disord* 2012; 27: 349–356.
  46. Aarsland D, Brønnick K, Larsen JP, *et al.* Cognitive impairment in incident, untreated Parkinson disease: the Norwegian ParkWest study. *Neurology* 2009; 72: 1121–1126.
  47. Aarsland D, Brønnick K, Williams-Gray C, *et al.* Mild cognitive impairment in Parkinson disease: a multicenter pooled analysis. *Neurology* 2010; 75: 1062–1069.
  48. Stern Y. Cognitive reserve and Alzheimer disease. *Alzheimer Dis Assoc Disord* 2006; 20: 112–117.
  49. Trojanowski JQ and Lee VMY. Parkinson's disease and related synucleinopathies are a new class of nervous system amyloidoses. *Neurotoxicology* 2002; 23: 457–460.
  50. Bullmore E and Sporns O. Complex brain networks: graph theoretical analysis of structural and functional systems. *Nat Rev Neurosci* 2009; 10: 186–198.
  51. Mori S and Zhang J. Principles of diffusion tensor imaging and its applications to basic neuroscience research. *Neuron* 2006; 51: 527–539.
  52. Müller H-P and Kassubek J. Diffusion tensor magnetic resonance imaging in the analysis of neurodegenerative diseases. *J Vis Exp* 2013; 77.
  53. Cope TE, Rittman T, Borchert RJ, *et al.* Tau burden and the functional connectome in Alzheimer's disease and progressive supranuclear palsy. *Brain* 2018; 141: 550–567.

Visit SAGE journals online  
journals.sagepub.com/  
home/tan

 SAGE journals